1868 *Inorg. Chem.* **1995,** *34,* 1868−1874

On the Structure of the $[XeOF_5]^-$ Anion and of Heptacoordinated Complex Fluorides Containing One or Two Highly Repulsive Ligands or Sterically Active Free Valence Electron Pairs[†]

Karl O. Christe,*,[1] David A. Dixon,[2] Jeremy C. P. Sanders,[3] Gary J. Schrobilgen,[3] Scott S. Tsai,[3] and William W. Wilson[1]

Rocketdyne, A Division of Rockwell International, Canoga Park, California 91309, Central Research and Development, Experimental Station, The DuPont Company, Wilmington, Delaware 19880-0328, and Department of Chemistry, McMaster University, Hamilton, Ontario L8S 4 MI, Canada

Received October 3, 1994[⊗]

The new $[XeOF_5]^-$ salt, $N(CH_3)_4XeOF_5$, was prepared. This highly explosive compound was characterized by infrared, Raman, and multinuclear NMR spectroscopy. The electronic structure, vibrational frequencies, and force field of the free $[XeOF_5]^-$ anion in C_{4v} and C_{5v} symmetry were calculated at the LDFT/PP/DZVP, NLDFT/PP/DZVP, HF/ECP/DZP, and MP2/ECP/DZP levels of theory. Except at the Hartree−Fock level, all of the calculations predict for free $[XeOF_5]^-$ a pseudooctahedral C_{4v} structure with a sterically inactive free valence electron pair on Xe to be lower in energy than a C_{5v} structure in which the oxygen and the sterically active free valence electron pair on Xe occupy the two axial positions of a pseudopentagonal-bipyramid. The vibrational spectra which were experimentally observed for solid $[XeOF_5]^-$ salts agree only with the spectra predicted from the C_{5v} model. The C_{5v} structure of $[XeOF_5]^-$ is analogous to those found for IF_7, $[IOF_6]^-$, and $[XeF_5]^-$, but differs from the distorted octahedral C_s structures found for XeF_6 and $[IF_6]^-$ and previously also proposed for $[XeOF_5]^-$. The preferences of heptacoordinated molecules for either pentagonal-bipyramidal or distorted octahedral structures and the fluxionality of some of these structures can be rationalized by the presence or absence of unequal ligand repulsion effects.

Introduction

The $XeOF_4$ molecule can form 1:1 and 3:1 complexes with strong Lewis bases, such as KF, RbF, CsF, and NOF.[4−6] The structure of the 3:1 complexes was established by X-ray crystallography and shown to contain the $[F(XeOF_4)_3]^-$ anion which consists of three $XeOF_4$ molecules bridged to a central $[F]^-$ anion.[7,8] For the $[XeOF_5]^-$ anion which is present in the 1:1 adducts, structure **I** of C_s symmetry was proposed[7,8] based on the observed Raman spectrum. The free valence electron pair on Xe was assumed to be sterically active and to occupy an XeF_3 face. This structural model was based on the structures found for XeF_6[9] and $[IF_6]^-$.[10] However, by analogy with the recently determined structures of $[XeF_5]^-$ [11] and $[IOF_6]^-$ [12] structure **II** of C_{5v} symmetry also needs to be considered for $[XeOF_5]^-$. This structure can be derived from that of $[XeF_5]^-$ by replacement of a sterically active free valence electron pair on Xe by a doubly bonded oxygen ligand.

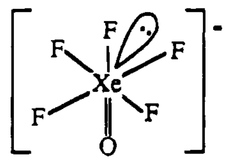

I (C_s)

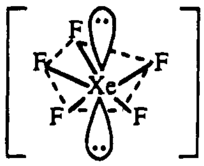

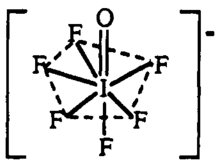

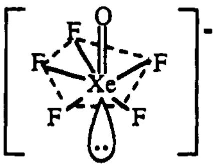

II (C_{5v})

Another structure for $[XeOF_5]^-$ which might also be of low energy is **III** in which the free valence electron pair on Xe is sterically inactive resulting in C_{4v} symmetry.

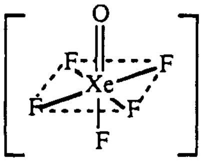

III (C_{4v})

It was, therefore, of interest, to reexamine the structure of the $[XeOF_5]^-$ anion. To minimize anion−anion interactions and to increase the solubility of the $[XeOF_5]^-$ salts for NMR

[†] Dedicated to Dr. Roland Bougon on the occasion of his 60th birthday.

[⊗] Abstract published in *Advance ACS Abstracts,* March 1, 1995.

(1) Rocketdyne. New address: Hughes STX, Phillips Laboratory Propulsion Directorate, Edwards Air Force Base, CA 93524, and Loker Hydrocarbon Research Institute, University of Southern California, Los Angeles, CA 90089.

(2) DuPont.

(3) McMaster University.

(4) Moody, G. J.; Selig, H. *Inorg. Nucl. Chem. Lett.* **1966**, *2*, 319.

(5) Selig, H. *Inorg. Chem.* **1966**, *5*, 183.

(6) Waldman, M. C.; Selig, H. *J. Inorg. Nucl. Chem.* **1973**, *35*, 2173.

(7) Schrobilgen, G. J.; Martin-Rovet, D.; Charpin, P.; Lance, M. J. *Chem. Soc. Chem. Commun.* **1980**, 894.

(8) Holloway, J. H.; Kaucic, V.; Martin-Rovet, D.; Russell, D. R.; Schrobilgen, G. J.; Selig, H. *Inorg. Chem.* **1985**, *24*, 678.

(9) Burbank, R. D.; Jones, G. R. *J. Am. Chem. Soc.* **1974**, *96*, 43.

(10) Majhoub, A. R.; Seppelt, K. *Angew. Chem., Int. Ed. Engl.* **1991**, *30*, 323.

0020-1669/95/1334-1868$09.00/0 © 1995 American Chemical Society

studies and possible growth of single crystals for X-ray diffraction, a larger countercation was desired. This prompted us to attempt the synthesis of $N(CH_3)_4XeOF_5$ and, if successful, to study its structure.

Experimental Section

Caution! The $XeOF_4-CH_3CN-N(CH_3)_4F$ system is hazardous and explosions have occurred several times when either rapidly cooling this system or handling solid $N(CH_3)_4XeOF_5$. Its handling should be limited to small quantities and appropriate safety precautions and shielding should be used at all times.

Materials and Apparatus. Literature methods were used for the syntheses of $XeOF_4$,[12] anhydrous $N(CH_3)_4F$,[13] and the $^{17,18}O$-enriched $XeOF_4$ (oxygen isotopic composition: ^{16}O, 36.5%, ^{17}O, 26.5%, and ^{18}O, 37.0%)[14] and the drying of CH_3CN.[15]

Acetonitrile was transferred in a flamed out Pyrex glass vacuum line that was equipped with Kontes glass–Teflon valves and a Heise pressure gauge. The oxidizers were handled in a stainless steel vacuum line equipped with Teflon–FEP U-traps, 316 stainless steel bellows-seal valves, and a Heise pressure gauge.[16] The metal line and the reactor were passivated before use with ClF_3, BrF_5 and XeF_6. Nonvolatile materials were handled in the dry nitrogen atmosphere of a glovebox.

The infrared, Raman, and MNR spectrometers that were used in this study have previously been described.[15] A Perkin–Elmer differential scanning calorimeter, Model DSC-1B, was used to determine the thermal stability of the salt. The samples were crimp-sealed in aluminum pans, and a heating rate of 10 °C/min in N_2 was used.

Synthesis of $N(CH_3)_4XeOF_5$. A $^3/_4$ in. o.d. Teflon–FEP ampule, which was closed by a stainless valve, was loaded in the drybox with $N(CH_3)_4F$ (1.724 mmol), and CH_3CN (7.35 mL) was added on the glass vacuum line. The ampule was connected to the steel vacuum line, and $XeOF_4$ (1.938 mmol) was added at −196 °C. The mixture was allowed to warm behind a blast shield to room temperature with occasional gentle agitation. All material volatile at 20 °C was pumped off for 4 h leaving behind a white solid (549 mg, weight calculated for 1.724 mmol of $N(CH_3)_4XeOF_5$ = 545.3 mg) that was identified by vibrational spectroscopy as $N(CH_3)_4XeOF_5$.

Computational Methods. A variety of electronic structure calculations were performed in order to calculate the geometries, relative energies, and vibrational frequencies of $[XeOF_5]^-$. The electronic structure calculations were done at four different levels and all calculations were done on a Cray YMP computer. The first set of calculations were done at the Hartree-Fock (HF/ECP/DZP) level with the program GRADSCF.[17] A polarized double-ζ valence basis set[18] (DZP) was used for all of the atoms with the inner shell electrons on Xe being treated by an effective core potential (ECP).[19] The geometries and frequencies at this level were calculated by using analytic derivative methods.[20,21] Calculations were then performed at the second order Møller-Plesset (MP2/ECP/DZP) level with only the valence electrons correlated.[22] The same basis set as used for the Hartree–Fock calculations was used for the MP2 calculations. The geometries were optimized and frequencies were calculated by numerical differentiation of the first derivatives at the MP2 level. The MP2 calculations were done with the program Gaussian92.[23] Density functional calculations were done with the program DGauss[24] at the local (LDFT) and nonlocal (NLDFT) (gradient-corrected) levels with two basis sets, one in which all of the electrons are included in a double-ζ valence-polarized (DZVP)[25] basis set and one in which the Xe core electrons are treated with a pseudopotential[26] (PP) and the remaining electrons are treated with a polarized valence double-ζ basis set. The local potential fit of Vosko, Wilk, and Nusair[27] was used at the local level (VWN/DZVP and VWN/PP/DZVP). The gradient corrected or nonlocal density functional calculations were done with the nonlocal exchange potential of Becke[28] together with the nonlocal correlation functional of Perdew[29] (BP/DZVP and BP/PP/DZVP). The geometries were optimized by using analytic gradient methods. The second derivatives at the all-electron, LDFT level (VWN/DZVP) were calculated analytically[30] whereas at the NLDFT level or when pseudopotentials were used the second derivatives were calculated by numerical differentiation of the analytic first derivatives. A two point method with a finite difference of 0.01 au was used.

Results and Discussion

Synthesis and Properties of $N(CH_3)_4XeOF_5$. The synthesis of $N(CH_3)_4XeOF_5$ was achieved according to reaction 1.

$$N(CH_3)_4F + XeOF_4 \xrightarrow[20\ ^\circ C]{CH_3CN} N(CH_3)_4XeOF_5 \qquad (1)$$

The compound is a white, highly sensitive solid that can explode when touched with a spatula. Rapid freezing of mixtures with CH_3CN has also resulted in explosions. Its thermal stability was examined by differential scanning calorimetry. It undergoes a strongly exothermic, violent decomposition at 145 °C. The compound's solubility in CH_3CN at 25 °C is very low and strongly decreases with decreasing temperature. This poor solubility in CH_3CN has limited the NMR studies to room temperature and has frustrated attempts to grow single crystals for an X-ray diffraction study.

---

(11) Christe, K. O.; Curtis, E. C.; Dixon, D. A.; Mercier, H. P.; Sanders, J. C. P.; Schrobilgen, G. J. *J. Am. Chem. Soc.* **1991**, *113*, 3351.

(12) Christe, K. O.; Wilson, W. W. *Inorg. Chem.* **1988**, *27*, 1296.

(13) Christe, K. O.; Wilson, W. W.; Wilson, R. D.; Bau, R.; Feng, J. *J. Am. Chem. Soc.* **1990**, *112*, 7619.

(14) Schumacher, G. A.; Schrobilgen, G. J. *Inorg. Chem.* **1984**, *23*, 2923.

(15) Christe, K. O.; Dixon, D. A.; Majhoub, A. R.; Mercier, H. P. A.; Sanders, J. C. P.; Seppelt, K.; Schrobilgen, G. J.; Wilson, W. W. *J. Am. Chem. Soc.* **1993**, *115*, 2696.

(16) Christe, K. O.; Wilson, R. D.; Schack, C. J. *Inorg. Synth.* **1986**, *24*, 3.

(17) GRADSCF is an ab initio program system designed and written by A. Komornicki at Polyatomics Research, Mountain View, CA.

(18) Dunning, T. H., Jr.; Hay, P. J. In *Methods of Electronic Structure Theory*; Schaefer, H. F., III, Ed.; Plenum Press: New York, 1977; Chapter 1.

(19) Wadt, W. R.; Hay, P. J. *J. Chem. Phys.* **1985**, *82*, 284.

(20) (a) Komornicki, A.; Ishida, K.; Morokuma, K.; Ditchfield, R.; Conrad, M. *Chem. Phys. Lett.* **1977** *45*, 595. (b) McIver, J. W., Jr.; Komornicki, A. *Chem. Phys. Lett.* **1971**, *10*, 202. (c) Pulay, P. In *Applications of Electronic Structure Theory*; Schaefer, H. F. III, Ed.; Plenum Press: New York, 1977; p 153. (d) Breidung, J.; Thiel, W.; Komornicki, A. *Chem. Phys. Lett.* **1988**, *153*, 76.

(21) (a) King, H. F.; Komornicki, A. *J. Chem. Phys.* **1986**, *84*, 5465. (b) King, H. F.; Komornicki, A. In *Geometrical Derivatives of Energy Surfaces and Molecular Properties*; Jorgenson, P., Simons, J., Eds.; NATO ASI Series C 166; D. Reidel: Dordrecht, The Netherlands, 1986; p 207.

(22) Frisch, M. J.; Trucks, G. W.; Schlegel, H. B.; Gill, P. M. W.; Johnson, B. G.; Wong, M. W.; Foresman, J. B.; Robb, M. A.; Head-Gordon, M.; Replogle, E. S.; Gomperts, R.; Andres, J. L.; Raghavachari, K.; Binkley, J. S.; Gonzalez, C.; Martin, R. L.; Fox, D. J.; Defrees, D. J.; Baker, J.; Stewart, J. J. P.; and Pople, J. A. *Gaussian 92/DFT, Revision F.3*; Gaussian, Inc.: Pittsburgh, PA, 1993.

(23) (a) Møller, C.; Plesset, M. S. *Phys. Rev.* **1934**, *46*, 618; (b) Pople, J. A.; Binkley, J. S.; Seeger, R. *Int. J. Quantum. Chem.*, *Quantum Chem. Symp.* **1976**, *10*, 1; Pople, J. A.; Krishnan, R.; Schlegel, H. B.; Binkley, J. S.; *Int. J. Quantum Chem.*, *Quantum Chem. Symp.* **1979**, *13*, 325; Handy, N. C.; Schaefer, H. F., III *J. Chem. Phys.* **1984**, *81*, 5031.

(24) (a) Andzelm, J.; Wimmer, E.; Salahub, D. R. In *The Challenge of d and f Electrons: Theory and Computation*; Salahub, D. R., Zerner, M. C., Eds.; ACS Symposium Series 394, American Chemical Society: Washington DC, 1989; p 228. (b) Andzelm, J. In *Density Functional Theory in Chemistry*; Labanowski, J., Andzelm, J., Eds.; Springer-Verlag: New York, 1991; p 155. (c) Andzelm, J. W.; Wimmer, E. *J. Chem. Phys.* **1992**, *96*, 1280. DGauss is a density functional program available via the Cray Unichem Project.

(25) Godbout, N.; Salahub, D. R.; Andzelm, J.; and Wimmer, E. *Can. J. Chem.* **1992**, *70*, 560.

(26) Chen, H.; Kraskowski, M.; Fitzgerald, G., *J. Chem. Phys.* **1993**, *98*, 8710; (b) Troullier, N.; Martins, J. L. *Phys. Rev. B* **1991**,*43*, 1993.

(27) Vosko, S. J.; Wilk, L.; Nusair, W. *Can. J. Phys.* **1980**, *58*, 1200.

(28) (a) Becke, A. D. *Phys. Rev. A* **1988**, *38*, 3098. (b) Becke, A. D. In *The Challenge of d and f Electrons: Theory and Computation*; Salahub, D. R., Zerner, M. C., Eds.; ACS Symposium Series 394; American Chemical Society: Washington DC, 1989; p 166. (c) Becke, A. D. *Int. J. Quantum Chem.*, *Quantum Chem. Symp.* **1989**, *23*, 599.

(29) Perdew, J. P. *Phys. Rev. B* **1986**, *33*, 8822.

(30) Komornicki, A.; Fitzgerald, G. *J. Phys. Chem.* **1993**, *98*, 1398 and references therein.

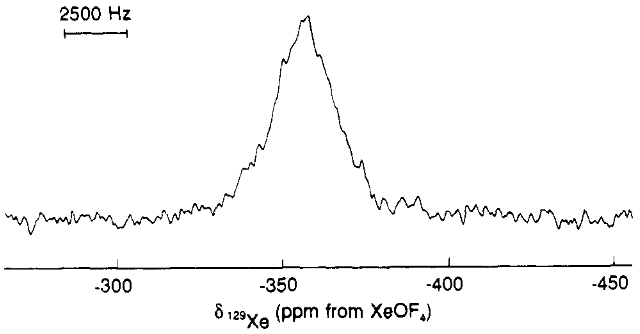

Figure 1. ^{129}Xe NMR spectrum (139.051 MHz) of a saturated solution of $N(CH_3)_4{}^+XeOF_5{}^-$ in CH_3CN at 30 °C.

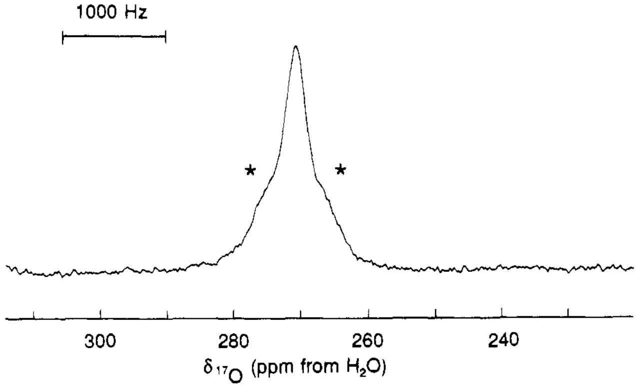

Figure 2. ^{17}O NMR spectrum (67.801 MHz) of a saturated solution of $N(CH_3)_4{}^+XeOF_5{}^-$ (oxygen isotopic composition: ^{16}O, 36.5%, ^{17}O, 26.5%, and ^{18}O, 37.0%) in CH_3CN at 30 °C.

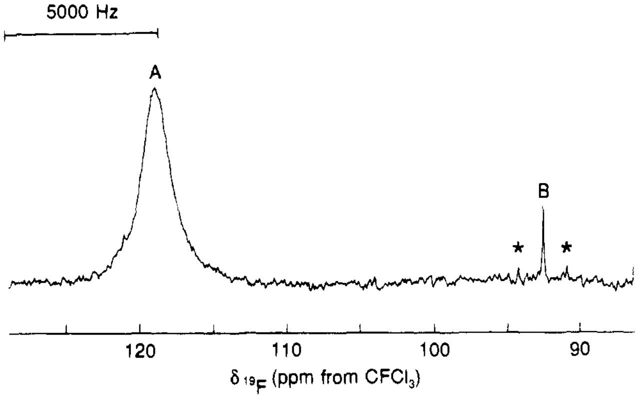

Figure 3. ^{19}F NMR spectrum (470.599 MHz) of a saturated solution of $N(CH_3)_4{}^+XeOF_5{}^-$ in CH_3CN at 30 °C: (A) $XeOF_5{}^-$; (B) $XeOF_4{\cdot}CH_3CN$. Asterisks denote ^{129}Xe satellites.

^{129}Xe, ^{17}O, and ^{19}F NMR Study of $XeOF_5{}^-$. The solubility of $N(CH_3)_4XeOF_5$ in CH_3CN was sufficient to allow the observation of ^{129}Xe, ^{17}O, and ^{19}F NMR spectra at room temperature.

The ^{129}Xe NMR spectrum of a saturated solution of $N(CH_3)_4XeOF_5$ (oxygen isotope composition: ^{16}O, 35.4%; ^{17}O, 21.9%; ^{18}O, 42.7%) in CH_3CN at 30 °C (Figure 1) reveals a broad singlet ($v_{1/2}$ = 2707 Hz) at $\delta(^{129}Xe)$ = 357.9 ppm. The lack of resolved spin–spin coupling to the five ^{19}F ligand nuclei can be attributed to intermolecular fluorine exchange which has also previously been observed, although to a much lesser extent, in the structurally related $[XeF_5]^-$ anion.[11] Attempts to reduce the rate of exchange by cooling the sample or by adding excess $N(CH_3)_4{}^+F^-$ were unsuccessful owing to the very low solubility of $N(CH_3)_4XeOF_5$ in CH_3CN below room temperature. The ^{129}Xe chemical shift is substantially more shielded (i.e., by −357.9 ppm) than that of neat $XeOF_4[\delta(^{129}Xe) = 0.0$ ppm]. This follows the expected trend of increased shielding with an increase in negative charge which is also observed for the ^{129}Xe shielding of $XeF_5{}^-$ with respect to that in XeF_4.[11,31]

The ^{17}O NMR spectrum of the same sample (Figure 2) shows a broad singlet ($v_{1/2}$ = 327 Hz) at $\delta(^{17}O)$ = 270.8 ppm. In addition, shoulders are observed at the base of the resonance which are attributed to natural abundance (26.44%) ^{129}Xe satellites and demonstrate the nonlability of the Xe=O bond. Gaussian deconvolution of the spectrum allows the extraction of $^1J(^{17}O-^{129}Xe)$ as 566 Hz. This coupling is significantly smaller than the $^1J(^{17}O-^{129}Xe)$ coupling in $XeOF_4$ and $[XeOF_3]^+$ (viz., 704 Hz[14] and 619 Hz,[32] respectively) which may be a consequence of the more polar bonds in the anion.

The ^{19}F NMR spectrum of a saturated solution of $N(CH_3)_4XeOF_5$ in CH_3CN at 30 °C (Figure 3) reveals two resonances: an intense broad singlet ($v_{1/2}$ = 975 Hz) at $\delta(^{19}F)$ = 118.9 ppm and a weak sharp singlet flanked by ^{129}Xe satellites [$^1J(^{19}F-^{129}Xe)$ = 1570 Hz] at $\delta(^{19}F)$ = 92.5 ppm. The broad resonance is attributed to the $[XeOF_5]^-$ anion with the fluoride ligands undergoing intermolecular exchange in agreement with the findings in the ^{129}Xe spectrum; the weak sharp resonance results from a small amount of solvated $XeOF_4$. The high frequency ^{19}F chemical shift of $[XeOF_5]^-$ with respect to $XeOF_4$ parallels the similar behavior of the ^{19}F chemical shifts of the pentagonal plane of F ligands in $XeF_5{}^-$ and $IOF_6{}^-$.[11,15] This chemical shift trend appears to be characteristic of a pentagonal planar arrangement of fluorine ligands around a heavy main-group atom[11,15,33] and indicates that the $[XeOF_5]^-$ anion adopts a pentagonal-bipyramidal structure, in agreement with the data from the vibrational spectra of $N(CH_3)_4XeOF_5$ (see below).

Vibrational Spectra and Electronic Structure Calculations. The vibrational spectra of $N(CH_3)_4XeOF_5$ were recorded and are summarized in Table 1. They are in good agreement with the Raman spectra previously reported[6-8] for $CsXeOF_5$ for which a distorted octahedral structure of C_s symmetry had been proposed.[7,8] In the absence of a crystal structure, the vibrational spectra were thoroughly analyzed to distinguish between the different possible structural models. Since the previously reported[6] Raman spectrum of $CsXeOF_5$ at low temperatures exhibited splitting into numerous extra bands,[7,8] the number of observed bands alone does not permit a positive distinction between the different symmetries of the proposed models. To overcome this problem, electronic structure calculations were carried out for $[XeOF_5]^-$ at a number of theoretical levels.

Before we discuss the calculations, we first describe our results on the model compound $XeOF_4$ whose structure and vibrational spectra are well-understood. Calculations were done at the HF/ECP/DZP, MP2/ECP/DZP, VWN/DZVP, VWN/PP/DZVP, BP/DZVP, and BP/PP/DZVP levels. The geometry results[33] are shown in Table 2 and the frequencies[34] are shown in Table 3. The geometry results show some interesting trends. The HF/ECP/DZP and MP2/ECP/DZP calculations predict the Xe=O bond to be too long by less than 0.02 Å. The Xe-F bond length is bracketed by the two methods with the HF results short by 0.02 Å and the MP2 value long by 0.055 Å. At the

---

(31) Jameson, C. J.; Mason, J. In *Multinuclear NMR*; Mason, J., Ed.; Plenum press: New York, 1987; Chapter 3, pp 66–68.

(32) Mercier, H. P. A.; Sanders, J. C. P.; Schrobilgen, G. J.; Tsai, S. S. *Inorg. Chem.* **1993**, *32*, 386.

(33) Jacob, E. J.; Bradford Thompson, H.; Bartell, L. S. *J. Mol. Struct.* **1971**, 8, 383 and references cited therein.

(34) Begun, G. M.; Fletcher, W. H.; Smith, D. F. *J. Chem. Phys.* **1965**, *42*, 2236; Tsao, P.; Cobb, C. C.; Claassen, H. H. *J. Chem. Phys.* **1971**, *12*, 5247 and references cited therein.

Table 1. Vibrational Spectra of the $XeOF_5^-$ Anion in Different Salts and their Assignments in point Group C_{5v} Compared to Those of the Closely Related $XeFe_5^-$ and IOF_6^- Anions and IF_7

assign (activity)	approx mode description	$XeOF_5^-$ (C_{5v})													XeF_5^- (D_{5h}) obsd freq, cm^{-1} (int (IR,Ra)^h)	IOF_6^- (C_{5v}) obsd freq, cm^{-1} (int (IR, Ra)^i)	IF_7 (D_{5h}) obsd freq, cm^{-1} (int (IR, Ra)^j)
		calcd freq, cm^{-1} (IR intens)							obsd freq, cm^{-1} (intens)							
		VWN/PP/DZVP		BP/PP/DZVP		MP2/ECP/DZP	HF/ECP/DZP		$N(CH_3)_4XeOF_5$^{e}		CsXeOF$_5$					
		unscaled	scaled	unscaled	scaled	unscaled	unscaled	scaled	IR 30 °C	Ra room temp and −150 °C	Ra^f room temp	RA ^{16}O^{g} −196 °C	RA ^{18}O^{g} −196 °C			
A_1(IR, Ra)	ν_1 ν Xe=O	904 (70)	870	865 (66)	904	950 (97)	759 (16)	759^d	878 ms	880 (32)	883(64)	883	839(66)		873 (vs, 53)	
	ν_2 ν sym XeF$_5$	535 (3)	515	478 (12)	500	465 (2.9)	593 (1.0)	516	516 m	515 (100)	525(100)	524	524(100)	502 (−, 100)	584 (−100)	635 (−, 100)
	ν_3 δ umbrella XeF$_5$	309 (35)	297	288 (36)	301	273 (61)	362 (84)	315	290 ms	296 (7)	290(7)	293	290(13)	290 (m, −)	359 (s, 4)	365 (s, −)
E_1(IR, Ra)	ν_4 ν as XeF$_5$	575 (671)	553	503 (604)	526	506 (813)	565 (1094)	492	495 vs			410 396 384 365	407(7) 390(24) 378(24) 352(15)	450 (vs, −)	585 (vs, −)	670 (vs, −)
	ν_5 δ wag Xe=O	367 (45)	353	342 (68)	358	343 (23)	407 (42)	354	370 m	370 sh	368(20)				407 (vs, −) 341 (−, 62) 260 (s, 2)	425 (vs, −) 319 (−, 6) 257 (w, −)
	ν_6 δ as in plane XeF$_5$	279 (8)	269	259 (17)	271	259 (12)	314 (4.3)	273	273 vw	270 sh	275(5)	274	267(8)	274 (s, −)		
E2(−, Ra)	ν_7 ν as XeF$_5$	458 (0)	441	430 (0)	460	406 (0)	511 (0)	445		470 (18) 450 (10)	469(35) 439(2)	473 468 435	473(34) 468(29) 435(12)	423 (−, 16)	530 (−, 4)	596 (−, 2)
	ν_8 δ sciss in plane XeF$_5$	417 (0)	401	376 (0)	393	376 (0)	463 (0)	403		397 (54)	397(47)	420 390 361	420(10) 390(40) 361(17)	377 (−, 23)	457 (−, 49)	510 (−, 17)
	ν_9 δ pucker XeF$_5$	119 (0)	115	97 (0)	101	87 (0)	148 (0)	129								

[a] Scaled by empirical factor of 0.9653 to maximize the fit with the observed frequencies. [b] Scaled by empirical factor of 1.0455. [c] Scaled by empirical factor of 0.8704. [d] Unscaled frequency value. [e] In addition to the listed bands, the following bands were observed. $N(CH_3)_4XeOF_5$: $XeOF_5^-$, Ra, 840 (4) = υ_7 (E_2) + υ_8 (E_2) = 847 (A_1 + A_2 + E_1) being in Fermi resonance with $\upsilon_1(A_1)$; 560 (2) = $2\upsilon_6$ (E_1) = 546 (A_1 + E_2) being in Fermi resonance with $\upsilon_2(A_1)$; Ir, 834 mw, ($\upsilon_7 + \upsilon_8$); 655 mw, ($\upsilon_6 + \upsilon_8$); $N(CH_3)_4^+$, Ra, 3054 (4), 3037 (2), 2990 (2), 2965 (3), 2930 (1), 1464 (12), 1416 (2), 1290 (1), 1178 (1), 951 (14), 759 (19), IR, 3050 mw, 2969 w, 1486 s, 1443 w, 1416 m, 1290 mw, 1178 w, 951 s, 455 sh. For the assignments of the $N(CH_3)_4^+$ bands, see refs 11, 13, 15, and 40 and references cited therein. [f] Data from ref 6. [g] Data from ref 8. [h] Data from ref 11. [i] Data from ref 15. [j] Data from ref 41.

Table 2: Observed and Calculated Geometries for $XeOF_4$

	experimental[35]	HF/ECP/DZP	MP2/ECP/DZVP	VWN/DZVP	VWN/PP/DZVP	BP/DZVP	BP/PP/DZVP
r(Xe=O), Å	1.7053 (0.00089)	1.720	1.722	1.786	1.676	1.814	1.688
r(Xe−F), Å	1.9040 (0.00002)	1.879	1.959	2.002	1.883	2.035	1.908
∠O=Xe−F, deg	91.66 (0.072)	90.6	92.7	92.6	92.4	92.7	92.7

Table 3: Observed and Calculated Vibrational Frequencies (cm^{-1}) and Infrared Intensities for $XeOF_4$

		expt[36]	intens (IR)	HF/ECP/DZP unscaled	HF/ECP/DZP scaled[a]	MP2/ECP/DZP unscaled	VWN/DZVP unscaled	VWN/PP/DZVP unscaled	BP/DZVP unscaled	BP/PP/DZVP unscaled
a_1	ν_1	926.3	s	778 (9.6)	778	1001 (62)	828 (28)	945 (44)	787 (26)	904 (40)
	ν_2	576.9	m	650 (1.3)	581	542 (3.4)	495 (3.2)	595 (2.4)	490 (3.5)	559 (2.4)
	ν_3	285.9	s	364 (72)	307	276 (48)	224 (32)	314 (30)	233 (31)	304 (29)
b_1	ν_4	543		614 (0)	549	511 (0)	467 (0)	544 (0)	464 (0)	501 (0)
	ν_5			239 (0)	202	180 (0)	141 (0)	211 (0)	153 (0)	203 (0)
b_2	ν_6	225		261 (0)	220	215 (0)	172 (0)	231 (0)	177 (0)	229 (0)
e	ν_7	609	vs	667 (772)	596	614 (478)	564 (410)	655 (481)	567 (381)	619 (461)
	ν_8	362	s	394 (27)	333	341 (19)	226 (13)	351 (23)	274 (12)	339 (10)
	ν_9	161		196 (0.5)	165	173 (5.6)	133 (3.1)	195 (0.8)	138 (3.7)	195 (0.7)

[a] Empirical scaling factors of 0.8947 and 0.8442 used for stretching and bending frequencies, respectively, ν_1 unscaled.

LDFT and NLDFT levels, neither all-electron calculation can reproduce the experimental geometry. However, the use of a pseudopotential on Xe leads to much better results. At both the LDFT and NLDFT levels, the Xe=O bond length is shorter than the experimental value. The VWN/PP/DZVP value for the Xe−F bond length is short by 0.02 Å whereas the BP/PP/DZVP result is slightly longer. The best prediction of the geometry is at the BP/PP/DZVP level. The vibrational spectra show some interesting trends. Although the Xe=O bond length is predicted reasonably well at the HF level, the Xe=O harmonic stretch is predicted to be too low by almost 150 cm^{-1}. Scaling the stretches (excluding the Xe=O stretch) at the HF level by 0.89 and the bends by 0.84 brings the results into better agreement with the experimental values. The MP2 level predicts the Xe=O stretch to be high by 75 cm^{-1}, consistent with the fact that the theoretical value is harmonic and the experimental value includes anharmonic effects. As would be expected based on the geometries, the DFT calculations with the DZVP basis set do a poor job at predicting the frequencies for $XeOF_4$. Use of the unscaled VWN values seems to give the best agreement with experiment. The only differences between the calculated and experimental values at the VWN level that are greater than 20 cm^{-1} are v_3, v_7, and v_9 with the largest error of 46 cm^{-1} found for v_7. On the basis of these results for $XeOF_4$, we only performed calculations on $[XeOF_5]^-$ with either pseudopotentials or effective core potentials at the HF, MP2, VWN, and BP levels.

The calculations on $[XeOF_5]^-$ were done for the C_{5v} (**II**) and C_{4v} (**III**) structures. An attempt to find a vibrationally stable structure of C_s symmetry for model **I** was unsuccessful. Both the C_{5v} (**II**) and C_{4v} (**III**) structures were found to be stable vibrational minima at all levels of theory except at the HF level where the C_{4v} structure essentially dissociated into $XeOF_4$ and $[F]^-$. In the three cases where correlation energy is included at some level in the calculation, the C_{4v} structure is actually predicted to be more stable than the C_{5v} structure by 15.1, 8.4, and 12.9 kcal/mol at the MP2, VWN and BP levels, respectively. The geometry parameters for $[XeOF_5]^-$ in C_{5v} symmetry are given in Table 4. By using appropriately chosen scale factors from $XeOF_4$, we can estimate an "experimental" structure of $[XeOF_5]^-$. The Xe=O bond distance is not predicted to change significantly from that in $XeOF_4$. However, there is a significant lengthening of the Xe−F bonds by 0.08 Å on addition of $[F]^-$ to $XeOF_4$. The Xe−F distance is predicted to be slightly shorter than the average value of r(Xe−F) = 2.01 Å found experimentally in the crystal for $[XeF_5]^-$.

Table 4. Calculated Geometries of $C_{5v}[XeOF_5]^-$

	HF/ECP/ DZP	MP2/ECP/ DZP	VWN/ECP/ DZVP	BP/ECP/ DZVP	predicted[a]
r(Xe=O), Å	1.733	1.737	1.691	1.703	1.72
r(Xe−F), Å	1.955	2.048	1.969	2.005	1.99
∠O=Xe−F, deg	91.0	92.8	92.2	92.6	92.2
∠F−Xe−F, deg	72.0	71.9	71.8	71.8	71.9

[a] Predicted values based on scale factors from $XeOF_4$ calculations.

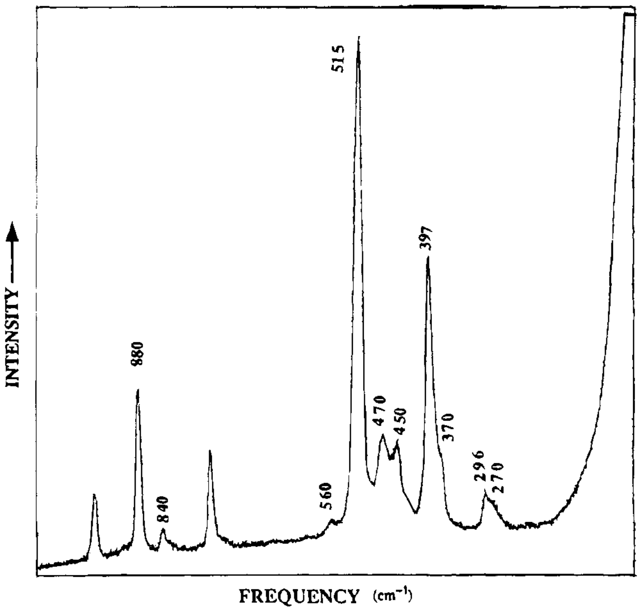

Figure 4. Raman spectrum of solid $N(CH_3)_4{}^+XeOF_5{}^-$ at 25 °C. The bands due to $XeOF_5{}^-$ are marked by their frequency values.

The vibrational spectra which were experimentally observed for the solid $XeOF_5{}^-$ salts (see Table 1 and Figure 4), are in accord only with the C_{5v} results and not with those[35] predicted for the energetically favored C_{4v} structure. This disagreement is deemed insignificant because (1) the energy differences between the C_{5v} and C_{4v} structures are not large; (2) the energies

---

(35) For example, the following geometry and unscaled vibrational frequencies (cm^{-1}) were obtained for C_{4v} $XeOF_5{}^-$ at the LDFT/ECP/DZVP level: r(Xe=O), 1.713 Å; $r(XeF_{eq})$ = 1.980 Å; $r(XeF_{ax})$ = 2.038 Å; $\angle OXeF_{eq} = 92.8$; $\angle F_{eq}XeF_{eq} = 89.8$; A_1, $v_1 = 873$ (167), $v_2 = 533$ (75), $v_3 = 417$ (88), $v_4 = 210$ (3); B_1, $v_5 = 406$ (O), $v_6 =$ 164 (O); B_2, $v_7 = 156$ (O); E, $v_8 = 525$ (640), $v_9 = 266$ (O), $v_{10} =$ 143 (O), $v_{11} = 124$ (O) (IR intensity in km/mol).

Table 5. Symmetry Force Constants[a] and Potential Energy Distribution[b] of C_{5v} $[XeOF_5]^-$ Calculated from the Scaled VWN/PP/DZVP (A_1 and E_2) and HF/ECP/DZP (E_1) Second Derivatives

	freq, cm^{-1}			sym force consts			
	obsd	calcd		F_{11}	F_{22}	F_{33}	PED
A_1	880	870	F_{11}	6.334			98.2 (1) + 1.8 (3)
	515	515	F_{22}	0.067	2.953		99.3 (2) + 0.3 (3)
	296	297	F_{33}	0.065	0.357	2.394	96.8 (3) + 2.7 (2) + 0.1 (1)
	freq, cm^{-1}			sym force consts			
	obsd	calcd		F_{44}	F_{55}	F_{66}	
E_1	495	492	F_{44}	2.030			91.7 (4) + 5.3 (6) + 2.9 (5)
	370	354	F_{55}	−0.358	2.183		85.0 (5) + 14.1 (6) + 0.9 (4)
	273	273	F_{66}	0.083	−0.182	0.906	54.4 (5) + 45.4 (6) + 0.1 (4)
	freq, cm^{-1}			sym force consts			
	obsd	calcd		F_{77}	F_{88}	F_{99}	
E_2	460	441	F_{77}	2.132			90.2 (7) + 9.5 (8)
	397	401	F_{88}	0.119	1.966		88.9 (8) + 10.6 (7)
	...	115	F_{99}	0.173	0.050	0.587	99.1 (9)

[a] Stretching constants in mdyn/Å, deformation constants in mdyn Å/rad^2, and stretch−bend interaction constants in mdyn/rad. [b] PED in percent.

Table 6. Comparison of the Stretching Force Constants (mdyn/Å) of $[XeOF_5]^-$ to Those of Similar Molecules and Ions

	$f_{Xe=O}$	$f_{r(XeF)}$	f_{rr}	$f_{rr'}$
$XeOF_5^-$	6.33	2.25	0.15	0.20
XeF_5^- [a]	...	2.10	0.14	0.22
$XeOF_4$[b]	7.08	3.26		
XeF_4[c]	...	3.06		

[a] Data from ref 11. [b] Data from ref 34. [c] Data from ref 39.

were calculated for the free gaseous $XeOF_5^-$ ion and not for solid $XeOF_5^-$ salts; (3) the electronic structure calculations at these levels of theory might not reliably predict effects as subtle as the steric activity of a free valence electron pair, and (4) the steric activity of a free valence electron pair of an ion in a solid salt can be strongly influenced by the nature of the counterion, as has been demonstrated[36] for the structurally closely related SeX_6^{2-} and TeX_6^{2-} salts. Depending on the symmetry of the crystal field, the free valence electron pair on the central atom of these anions can be sterically either active or inactive. As an example of the difficulty in predicting the geometry of these ions, we calculated the electronic structure of the isoelectronic $[IF_6]^-$ ion. At the HF level,[37] it has been shown that the structure with C_{3v} symmetry is lower in energy by 23.5 kcal/mol compared to the O_h structure and the C_{2v} symmetry structure is 21.6 kcal/mol lower in energy than the octahedral structure. This result is consistent with the experimental measurements on this compound.[10,38] At the VWN/PP/DZVP level, $[IF_6]^-$ is predicted to be very close to an octahedron although there may be a slight distortion to C_{3v} symmetry. Beginning from a structure of C_{2v} symmetry, the structure collapsed to a structure of O_h symmetry whereas beginning from C_{3v} symmetry, the structure relaxed to a nearly octahedral structure with C_{3v} symmetry which is only 0.5 kcal/mol more stable than the O_h structure. A structure of C_{5v} symmetry was found to be a minimum for $[IF_6]^-$ but was found to be 16.0 kcal/mol less stable than the structure of near O_h symmetry.

A normal coordinate analysis was also carried out for $[XeOF_5]^-$ in point group C_{5v}. The nine fundamental vibrations can be classified as $\Gamma = 3A_1(IR, Ra) + 3E_1(IR, Ra) + 3E_2(Ra)$. The internal coordinates and symmetry coordinates used for $[XeOF_5]^-$ are analogues to those previously given for the closely related $[XeF_5]^-$ [11] and $[IOF_6]^-$ [15] anions. The symmetry force constants and the potential energy distribution for $XeOF_5^-$ are summarized in Table 5. The listed force field is based on the A_1 and E_2 blocks from the VWM/PP/DZVP calculation and the E_1 block from the HF/ECP/DZP calculation because their scaled frequencies showed the smallest deviations from the experimental values. The use of symmetry blocks from two different sets of calculations is permissible since the symmetry blocks are completely independent of each other. The internal stretching force constants of $[XeOF_5]^-$ are compared in Table 6 to those of closely related molecules[11,34,39] and ions and exhibit the expected trends; i.e., the addition of a negatively charged $[F]^-$ ligand to $XeOF_4$ or XeF_4 causes a weakening of both the Xe=O and the Xe−F bonds due to an increase of the polarities of the Xe−ligand bonds. The addition of an oxygen ligand to $[XeF_5]^-$ or XeF_4 results in a slight strengthening of the Xe−F bonds, but the effect is small and indicates that the electron withdrawing effect of the oxygen ligand is weak; i.e., the effective electronegativities of the oxygen ligand and the $[XeF_5]^-$ or XeF_4 groups must be similar.

Discussion

The above results and their analysis strongly support for $[XeOF_5]^-$ a pseudopentagonal-bipyramidal structure of C_{5v} symmetry with a localized free valence electron pair on Xe. This structure is analogous to those known for $[XeF_5]^-$ and $[IOF_6]^-$ but differs from that of free XeF_6 which is a highly fluxional, dynamically distorted octahedron with six fluorine ligands and a delocalized sterically active free valence electron pair on xenon. This raises the question as to what causes this different behavior of the free valence electron pair in these heptacoordinated species. The following rationale provides a ready answer. If in a heptacoordinated species all seven ligands are identical, as for example in IF_7,[40] $[TeF_7]^-$, or $[XeF_7]^+$,[41] the resulting structure is a highly fuxional pentagonal-bipyramid in which axial and equatorial ligands can easily exchange positions. If one of the seven ligands is replaced by a more repulsive or space filling ligand, such as a doubly bonded oxygen atom in $[IOF_6]^-$,[15] this more repulsive ligand will be restricted to one of the less crowded axial positions because a positional exchange with an equatorial ligand is energetically unfavorable. This results in a rigid structure of C_{5v} symmetry. If, however, this more repulsive ligand is a free valence electron pair which can be easily delocalized, the resulting structure can readily undergo dynamic distortion and intramolecular fluorine exchange and one obtains the dynamically distorted octahedral XeF_6 type structures. Another example of this type of structure is $[IF_6]^-$.[10,38] This type of structure, however, is only observed if there is enough room around the central atom for seven ligands. If the maximum coordination number is reduced to

---

(36) Abriel, W. *Acta Crystallogr., Sect. B* **1986**, *B42*, 449.
(37) Klobukowski, M.; Huzinaga, S.; Seijo, L.; Barandiarán, Z. *Theor. Chim Acta* **1987**, *71*, 237.
(38) (a) Christe, K. O.; Wilson, W. W. *Inorg. Chem.* **1989**, *28*, 3275. (b) Christe, K. O. *Inorg. Chem.* **1972**, *11*, 1220.
(39) Christe, K. O.; Naumann, D. *Inorg. Chem.* **1973**, *12*, 59.
(40) Christe, K. O.; Dixon, D. A.; Sanders, J. C. P.; Schrobilgen, G. J.; Wilson, W. W. *J. Am. Chem. Soc.* **1993**, *115*, 9461.
(41) Christe, K. O.; Curtis, E. C.; Dixon, D. A. *J. Am. Chem. Soc.* **1993**, *115*, 1520.

six, as in $[ClF_6]^-$ [42] or $[BrF_6]^-$,[38,43,44] the free valence electron pair becomes sterically inactive resulting in a rigid octahedron.

Replacement of two fluorine ligands in XF_7 by more repulsive ligands invariably leads to a rigid pentagonal bipyramid since these two ligands can minimize their mutual repulsion by occupation of the two opposing axial positions. Typical examples for such cases are either $[XeF_5]^-$,[11] which possesses two free valence electron pairs on Xe, or $[XeOF_5]^-$, which possesses one free pair and one doubly bonded oxygen ligand. This rationale can account for all the experimentally observed geometries and the presence or absence of fluxionality in these heptacoordinated species and, for the isolated species, allows the following general predictions where E and R signify free valence electron pairs and more repulsive ligands, respectively.

XF_7	fluxional pentagonal-bipyramid
XF_6E	fluxional distorted octahedron
XF_5E_2	semirigid pentagonal-bipyramid with two axial free electron pairs
XF_6R	rigid pentagonal-bipyramid with a more repulsive axial ligand
XF_5R_2	rigid pentagonal-bipyramid with two more repulsive axial ligands
XF_5ER	rigid pentagonal-bipyramid with a more repulsive axial ligand and axial-free electron pair

Acknowledgment. The work at Rocketdyne was financially supported by the U.S. Army Research Office and the U.S. Air Force Phillips Laboratory and that at McMaster University by the Natural Sciences and Engineering Research Council of Canada and the U.S. Air Force Phillips Laboratory.

IC941126Y

---

(42) Christe, K. O.; Wilson, W. W.; Chirakal, R. V.; Sanders, J. C. P.; Schrobilgen, G. J. *Inorg. Chem.* **1990**, *29*, 3506.

(43) Bougon, R.; Charpin, P.; Soriano, M. *C. R. Acad. Sci., Ser. C* **1972**, *272*, 565.

(44) Mahjoub, A. R.; Hoser, A.; Fuchs, J.; Seppelt, K. *Angew. Chem., Int. Ed. Engl.* **1989**, *28*, 1526.